Sustainable Cities and Society 52 (2020) 101824

Contents lists available at ScienceDirect

Sustainable Cities and Society

journal homepage: www.elsevier.com/locate/scs

Optimal sizing and techno-economic analysis of grid-connected nanogrid for tropical climates of the Savannah

Ahmed Tijjani Dahiru[a,b], Chee Wei Tan[a,*]

[a] Division of Electrical Power Engineering, School of Electrical Engineering, Faculty of Engineering, Universiti Teknologi Malaysia, 81310, Skudai, Johor, Malaysia
[b] Department of Electrical and Electronics Technology, FCE (Technical) Bichi, Kano, Nigeria

ARTICLE INFO

Keywords:
Renewable energy
Nanogrids
Optimizations
Cost of energy
Net present cost
Greenhouse gas emission
Renewable fraction

ABSTRACT

Reliability and costs are mainly considered in performance analysis of renewable energy-based distributed grids. Hybrid Optimization of Multiple Energy Renewables was used in techno-economic analysis of renewable energy systems involving photovoltaics, wind, diesel and storage in tropical regions of Amazon, Central Asia and Mediterranean. In a study for a Guinea Savannah region, 70% of renewable energy fraction was achieved. However, levelized cost of energy of 0.689 $/kWh was higher than tariff rate of 0.6 $/kWh. This paper considers Hybrid Optimization of Multiple Energy Renewables to achieve lower levelized cost of energy and net present costs of a nanogrid for increased reliability and low per capita energy consumption of 150 kWh in a Sudan Savannah region of Nigeria. The proposed grid connected nanogrid aims to serve daily residential demand of 355 kWh. A range of 0.0110 $/kWh to 0.0095 $/kWh and $366,210 to $288,680 as negative values of levelized cost of energy and net present cost respectively were realized, implying potentials for a large grid export. The renewable energy fraction of up to 98% was also achieved in addition to low greenhouse gas emission of 2,328 tons/year. The results may further be consolidated with strategies for power dispatch and load scheduling.

1. Introduction

The uncertainties in the global energy markets, the environmental implications of the fossil fuel combustions and high level of power losses continue to be a threat to the prospects of conventional power grids. The large economies of western countries, Asia and Middle East utilize the potentials of the renewable energy (RE) resources available within their locations to reduce socioeconomic implications of traditional fossil fuel power generations. The less economically advantaged societies of Africa, South America and the Caribbean and Central Asia are naturally endowed with adequate solar, wind and water resources to supplement the persistent energy deficits using an emerging technology of clean energy production. Yet, the limited economic strength of the countries within the regions is an impediment to realization of energy goals in both fossil fuel and renewable resources. However, intermittence of RE resources is challenging to the prospects of RE system integration into power grids. These implies that optimization methods and strategies are important to feasibility of RE generation in today's power system grids.

Different optimization methods are considered in finding optimal solutions to planning and operation of RE-based or RE-integrated systems. In reference Momoh (2012), optimization techniques are being classified into five. The five distinctive optimization classes categorized into more general concept of optimization classifications are shown in Fig. 1. It is worthy of note that adaptive dynamic programming, evolutionary programming and intelligent methods are classified into artificial intelligence (AI) category of optimization methods for clarifications based on their bio-inspired characteristics.

Sizing of components is a major aspect of power grid planning. Optimization for sizing in power grids refers to economic selection of system's components (as inputs) for the purpose of achieving best possible technical and/or economic performance objectives (as outputs). Sizing of components in a distributed generation (DG) system involves selection of component specifications depending on load to be served. Issues such as unmet demands and dump energies resulting from supply shortage and non-curtailed and/or oversized system respectively are examples of uneconomic performance of a system. Various methods were used in literature to optimize RE-based power systems for economy and reliability. Sizing methods implemented using classical algorithms include grid connected microgrid's battery energy storage system (BESS) to assess the economic performance using Linear Programming in (Sukumar, Mokhlis, Mekhilef, Naidu, & Karimi, 2017). Islanded hybrid microgrid is designed to consists of power, cooling, hydrogen storage and load (Li, Roche, Paire, & Miraoui, 2017). A multi-

* Corresponding author.
E-mail address: cheewei@utm.my (C.W. Tan).

https://doi.org/10.1016/j.scs.2019.101824
Received 31 January 2019; Received in revised form 3 September 2019; Accepted 4 September 2019
Available online 17 September 2019

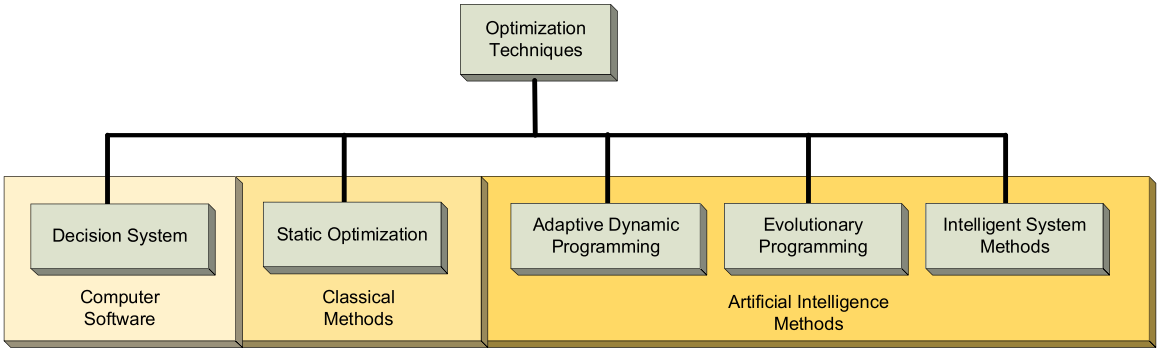

Fig. 1. Classifications of optimization techniques used in modern power grids.

objective sizing problem was decomposed and solved using Nash Bargain method, where cost of operation and carbon emission were reduced by 15.7% and 12.9% respectively (Zenginis et al., 2017). Mixed integer linear programming (MILP) was proposed in (Strnad & Prenc, 2017) and (Akram, Khalid, & Shafiq, 2018) to find optimal sizes in system with DG unit and battery based on operational savings and investment cost objectives. An analytical methods of Loss of Power Supply Probability (LPSP) and Reliability Improvement Method (RIM) was used in (Ayop, Isa, & Tan, 2018) to size a photovoltaic (PV) only standalone nanogrid for a university building. Only 4.9% was realized by the LPSP, whereas the RIM was able to improve the system by 77.8%. A cost-effective energy storage was sought in (Jacob, Banerjee, & Ghosh, 2018). Hence, pinch analysis and design space for a hybrid storage were proposed as generic sizing methodology. A cyber-physical Energy Management (EM) and sizing commitment for a networked nanogrids were implemented in (Ban, Shahidehpour, Yu, & Li, 2017) for improved cost and reliability. MILP was also used for capacity sizing of generating components and storage. A joint capacity optimization was proposed in (Akram et al., 2018) to reduce initial and running costs for a community-based PV/Wind/Diesel and Energy Storage System using labyrinthine optimizations to size generating components and loads.

The AI-based optimization methods involve techniques implemented using intelligent systems. Example of such implementations is multi-objective optimal sizing of a storage in Electric Vehicle, where GA based Fuzzy Logic Control were used to improve and predict the dynamic life span of the battery storage (Rahbari et al., 2017). A Multi-objective particle swarm optimization (PSO) was developed to balance the benefits of cost and reliability in a microgrid (Borhanazad, Mekhilef, Gounder Ganapathy, Modiri-Delshad, & Mirtaheri, 2014). Sizing is proposed using adaptive nesting evolutionary algorithm for a grid-connected microgrid, made up of PV, wind and BESS. Results obtained were compared with that obtained from a two-step algorithm, where 3.5% improvement was achieved (Mallol-Poyato, Jiménez-Fernández, Díaz-Villar, & Salcedo-Sanz, 2017). Hybrid storage of Lead-Acid and Lithium-ion batteries and supercapacitors were sized in order to optimize microgrid scheduling due to uncertainties of the natural resources, hence, utilized PSO to obtain sizing parameters of Lifecycle cost (LCC), construction cost, operation and maintenance costs (Liu, Chen, Zhuo, & Jia, 2017). An autonomous community microgrid planning in (Hussain, Arif, Aslam, & Shah, 2017) considers siting and sizing of tri-generation equipment. The results obtained from PSO-based solutions were tested on standard IEEE 33-bus distribution.

There are implementations of software-based optimizations in literature that were considered to be faster and more versatile than the developed classical or AI-based optimization methods. Most of the software-based optimizations implemented used Hybrid Optimization of Multiple Energy Renewables (HOMER). However, some studies consider other optimization software such as TRNSYS in (Atia & Yamada, 2016) and OPENDSS in (Sepulveda, Camilo, & Mauricio, 2018). Field-on-Lab Demonstration for a PV/Wind/Battery nanogrid was analyzed by simulations in HOMER environment and tested by hardware (Tudu, Mandal, & Chakraborty, 2018). Against the obstacles of distance, economy and official bureaucracies, electric nanogrid is proposed for a rural electrification of an energy-poor community by analyses and load aggregation in HOMER. Another nanogrid sizing considers an estimated and measured weather data for comparison in sizing of a PV/Wind/Battery grid-connected hybrid. Lower Levelized Cost of Energy (LCOE) of 0.15 $/kWh against the unit tariff of 0.175 $/kWh was realized hence, the results obtained corresponds to lower Net Present Cost (NPC) for a 25-year investment (Sadati, Jahani, Taylan, & Baker, 2018). A study in (Sepulveda et al., 2018) also considers HOMER in sizing of a DG system made up of PV cells and wind turbine (WT) system to be integrated with a distribution system. HOMER and Internet of Things (IoT) smart systems were used in designing a PV-based nanogrids based on requirements of a Middle East climate. The main objective of the work was to use IoT for monitoring and control of power consumptions. Hence, PV cells and batteries were sized based on location's load profiles (Akmal, El Kashif, Ghazal, & Al Tarabsheh, 2016). HOMER was used to implement nanogrid design, as a standalone system to achieve 100% availability of electricity supply to an energy-poor village in Central Nigeria (Akinyele, 2017). The RE fraction achieved was up to 70%. However, the LCOE of 0.628 $/kWh obtained from the system was comparatively higher than the retail price 0.6 $/kWh, while the greenhouse gas (GHG) emissions not being addressed.

In this paper, it is envisaged that the 150 kWh average per capita electricity consumption in Nigeria can be improved using a nanogrid system design for a suburban quarter of Danladi Nasidi in Kano Nigeria using HOMER-Pro optimizer. The nanogrids as a scaled down system of microgrids may be a formation of a confined electricity supply system to serve limited area or specific application while in isolation or in connection to the main grid that differ in designs, types or size of loads they deliver (Burmester, Rayudu, Seah, & Akinyele, 2017; Paper & Boer, 2013). Thus, having microgrids concepts in mind, configuration for nanogrids may be easier to comprehend. What needs to be considered are the types and sizes of loads and location's RE resources. These mainly determines nanogrid's type and size, as DC nanogrids, AC nanogrids or hybrid system (Burmester et al., 2017). The performance of the proposed nanogrid under six different component configurations in terms of lower LCOE and NPC were analyzed and were found have negative value ranges of 0.0110 $/kWh to 0.0099 $/kWh and $366,840 to $290,100 $290,100 respectively from the first four out of the six configurations analyzed. This indicates a good prospect for grid penetration (Bachner, Tuerk, Williges, & Steininger, 2017; Ueckerdt, Hirth, Luderer, & Edenhofer, 2013). In addition to the economic achievements, the RE fraction of up to 98% was also realized with a relatively high GHG emissions rates.

Table 1
Extract of some of the most recent optimizations implemented with HOMER.

Ref	System	Components	Climate	Autonomy	NPC ($)	LCOE ($/kWh)	RE Fraction (%)	GHG Emission (tons/yr)
(Tudu, Mandal, & Chakraborty, 2018)	Nanogrid	PV/wind/Battery	Tropical Central Asia	Grid connected	20,790	0.673	–	–
(Akinyele, 2017)	Nanogrid	PV/Wind/Diesel/Battery	Tropical Guinea Savannah	Standalone	50,593 – 133,560	0.315 – 0.689	70	–
(Sadati, Jahani, Taylan, & Baker, 2018)	Nanogrid	PV/Wind/Battery	Tropical Mediterranean	Grid connected	38,014,856 – 38,3400	0.150 – 0.145	36 – 38	4000
(Sepulveda, Camilo, Canha Luciane, & Sperandio Mauricio, 2018)	Nanogrid	PV/Wind/Battery	Tropical Amazon	Grid connected	11,828,490 – 30,978,762	0.061 – 0.188	–	–
(Abdilahi et al., 2014)	Microgrid	PV/Wind/Diesel	East African Tropics	Autonomous	22,99,519	0.408	58	–
(Isa, Das, Tan, Yatim, & Lau, 2016)	Nanogrid	PV/Diesel/Fuel Cell/Battery/Hydrogen Tank	Tropical Rain Forest	Grid connected	1,06,551	0.091	0.82	25.873
(Boussetta, El Bachtiri, Khanfara, & El Hammoumi, 2017)	Microgrid	PV/Wind	Tropical Mediterranean	Grid connected	2,10,000	0.090 – 1.117	19 – 72	50

2. The reference case analysis

Performance of the standalone system considered in (Akinyele, 2017) is robust in terms of RE fraction and availability as indicators of system reliability. However, higher LCOE as economic indicator and unaddressed GHG emission remain to be issues. In the proposed configurations, grid connection substituting diesel set used in referred study in reference (Akinyele, 2017) is envisaged to at least maintain the same RE fraction and most likely reduce the LCOE significantly. The unreported GHG emission in the referred work shall be considered in the proposed system's analysis to compare within the global averages.

Location based optimization cases summarized in Table 1 indicates performance of RE based systems implemented for reliability and economy. Most of the locations are tropical regions such that solar insolation and moderate wind speeds are much available (E. (International R. E. A.-I. Aberg et al. (2018); International Renewable Energy Agency, 2014). Hence, PVs and WTs are mostly used as generating components. Over a half of the works consulted were standalone systems, but the most important aspect of interest is the wide margin in between the performance parameters. While the NPC obtained were few hundred thousand United States dollars (US$) in some of the result analysis, others run into tenths of millions of US$, which could be attributed to size variations and hence justified. The LCOE differences however, shall be considered comparatively for analysis. Considering the most expensive LCOE realized in (Akinyele, 2017), different operating conditions were analyzed, and hence 0.315 $/kWh to 0.689 $/kWh is the highest so far obtained from the analyses. The RE fraction of 70% may be considered adequate however, GHG emission is not reported and hence, considered not part of the reference study's investigations. Diesel plant being part of the reference case power sources is responsible for the remaining 30% system's power contribution whose knowledge of the emission rates should be considered important to the study analysis. The summary presented in Table 1 indicates parameters used mainly in performance analysis in literature, that mainly consider NPC, LCOE, RE fraction and GHG emission rates being expressed in Eqs. (1), (2) and (3) which are also used in the case study analysis. Other parameters considered in various analysis include plant availability, performance ratio, internal rate of return, return on investment, the net present value and peak-average-ratio.

The NPC as a main parameter, also referred to as the LCC for a project is considered as the difference between costs incurred towards installation, maintenance, operation and replacement costs and all revenues realized over the entire project life time (Akinyele, 2017; HOMER ENERGY, 2018; Sadati, Jahani, Taylan, & Baker, 2017). This can mathematically be represented by the given Eq. (1), where C_t is the annual cost for t series of investment years, n as the total number of years for the project lifetime and r as the annualized discount rate.

$$NPC = \sum_{t=1}^{n} \frac{C_t}{(1+r)^t} \tag{1}$$

The LCOE is another major economic indicator in system analysis as the average cost incurred to produce per unit kWh of useful electricity. Note that LCOE does not cover energy needs in serving thermal loads (Akinyele, 2017; HOMER ENERGY, 2018; Sadati et al., 2017). The mathematical expression for determining LCOE is given in Eq. (1), where C_G C_B H_S and E_S are the annualized cost of electricity generation, total marginal cost of boiler, the total heat served and the total electricity served respectively.

$$LCOE = \left(\frac{C_G - C_B H_S}{E_S} \right) \tag{2}$$

The GHG emission is a derivative of technical performance resulting from combustion of fossil fuels in energy generation. Reference Boussetta, El Bachtiri, Khanfara, and El Hammoumi (2017) categorizes carbon dioxide (CO_2), Sulphur Dioxide (SO_2) and Nitrogen oxide (NOx)

Table 2
Energy consumptions from selected residential buildings of Danladi Nasidi Quarters.

Appliances	Power Ratings (W)	Household 1		Household 2		Household 3		Household 4		Household 5	
		Quantity	Daily usage (Hours)	Quantity	Daily usage (Hours)	Quantity	Daily usage (Hours)	Quantity	Daily usage (Hours)	Quantity	Daily usage (Hours)
Lightings	18	11	8	10	12	25	12	25	12	12	6
Fridge	450	1	24	–	–	2	24	1	24	1	24
A/C	900	3	8	1	6	3	14	–	–	–	–
TV set	330	2	12	1	12	3	16	1	16	1	16
Water pump	750	1	1	–	–	1	1	1	1.5	1	1
Electric iron	1000	1	1	1	1	1	1	1	2	–	–
Blender	250	1	0.17	–	–	1	0.5	–	–	1	0.08
Washing machine	1900	1	0.75	1	1	1	1.5	–	–	–	–
Ceiling fan	90	5	16	3	16	3	16	9	16	3	16
Rice cooker	450	–	–	1	0.75	–	–	–	–	–	–
Standing fan	50	1	16	2	16	1	16	–	–	1	16
Electric kettle	2000	–	–	1	0.3	–	–	–	–	1	0.5
Microwave oven	1200	–	–	–	–	–	–	–	–	1	0.08

among the pollutants expected from a PV/Wind hybrid systems. Whereas Methane (CH4) is another pollutant but insignificantly contributes to emissions in power generation. The RE fraction is obtained from percentage contribution of the participating RE components within a projects per total energy generation. Hence, Eq. (3) as contained in Boussetta et al. (2017) is provided for calculating the values of the fraction, where f_{RE} is the RE fraction, E_{NR} is the non-RE production and E_{SER} is the total energy served.

$$f_{RE} = \left(1 - \frac{E_{NR}}{E_{SER}}\right) \tag{3}$$

3. Case study

In the proposed study, nanogrid comprising of five housing units in Danladi Nasidi quarters, Kano Nigeria is aimed to be designed using PV and WT as generating components. The proposed grid-connected system is expected to be supported by a battery storage for added reliability against periods of autonomous operations. Table 2 shows electrical loads for the five selected houses based on 24-h demands as obtained from consumer load survey upon which the proposed system design shall be based. HOMER optimization software is considered for the analysis to evaluate techno-economic performance parameters of NPC, LCOE, RE fraction and GHG emission, being expressed in Eqs. (1)–(3). The method is chosen for the study due to its speed and versatility (support for numerous RE generating sources and different operating topologies). The area is located within 11°, 56.38`N and 8°, 37.07`E latitude, and falls around the center of northern Nigeria's Sudan Savannah region, where the average solar radiation hours are up to 11.5 (Honsberg & Bowden, 2019).

4. The nanogrid system design

The proposed grid-connected nanogrid design whose location's weather data of solar radiation, ambient temperature and wind speeds are shown in Figs. 3 and 4, comprises of generating system, power converters and storage to be sized based on the 24 -h maximum demands shown in Fig. 2. There are different sensitivity cases in selection of components based on specifications for optimal configurations of generating components, BESS, power converters and main grid coupling. The main implications in the sensitivity analysis is the wide range of technical and economic performance options to be realized, which shall be the basis of most optimization commitments. Schematics of Fig. 5 illustrates the system's architecture as an overall arrangement of components and parts of the nanogrid, upon which configurations based on capacity size shall be determined by Eqs. (4)–(11) (Boussetta et al., 2017).

4.1. The case study load profiles

The case study location's energy consumptions summarized in Table 2 consists of electrical and thermal loads meant for domestic purposes. This indicates the location's consumer category of residential system. The contents of the Table highlight the appliances' power ratings, quantity in use for each household and estimates of daily usage. The hourly distribution of the load is also presented graphically in Fig. 2 for a 24-h consumption cycle, where maximum demand is 355 kW h and peak for 24-h profile is about 42 kW.

4.2. The system components and structure

The reference study whose results is aimed to be benchmarked is the nanogrid design and analysis carried out in Akinyele (2017). Both the reference and the proposed designs are analyzed in HOMER for optimized configurations however, major differences between the two are the autonomous architecture of the reference, the grid connection in the proposed nanogrid design and the climatic conditions of the two locations. The nanogrid is proposed to be connected to the main grid system that supplies the case study location in vertically structured conventional grid system equipped with a 500kVA, 33 kV/415 V feeder. The illustrations of Fig. 5 show the structure the proposed nanogrid comprising of the following RE based components;

(a) The solar photovoltaic system

The configurations for the PV depend on commercially available specifications such as the rated power, lifespan as well as efficiencies obtained from datasheets (Tycon Solar, 2018). The capital and replacement costs are important to economic performance analysis, as summarized in Table 3. Energy generated from the PV cells for time (t), that falls within theoretical frameworks of Eqs. (4) and (5) as obtained in (Atia & Yamada, 2016), where T_C is the temperature of the cell in °C, T_{NO} is nominal operating cell temperature in °C, I_{GR} is the incident solar radiation (kW/m^2), T_a is the ambient temperature in °C, I_{ST} is the standard radiation (kW/m^2), k_p is the power temperature coefficient (%/°C) and T_{STC} is the standard test condition cell temperature (°C).

$$T_C(t) = T_a(t) + I_{GR}(t)\frac{NOCT - 20}{0.8} \tag{4}$$

$$P_{PV}(t) = Y_d \frac{I_{GR}(t)}{I_{ST}}\left[1 - \frac{K_p}{100}(T_C(t) - T_{STC})\right] \tag{5}$$

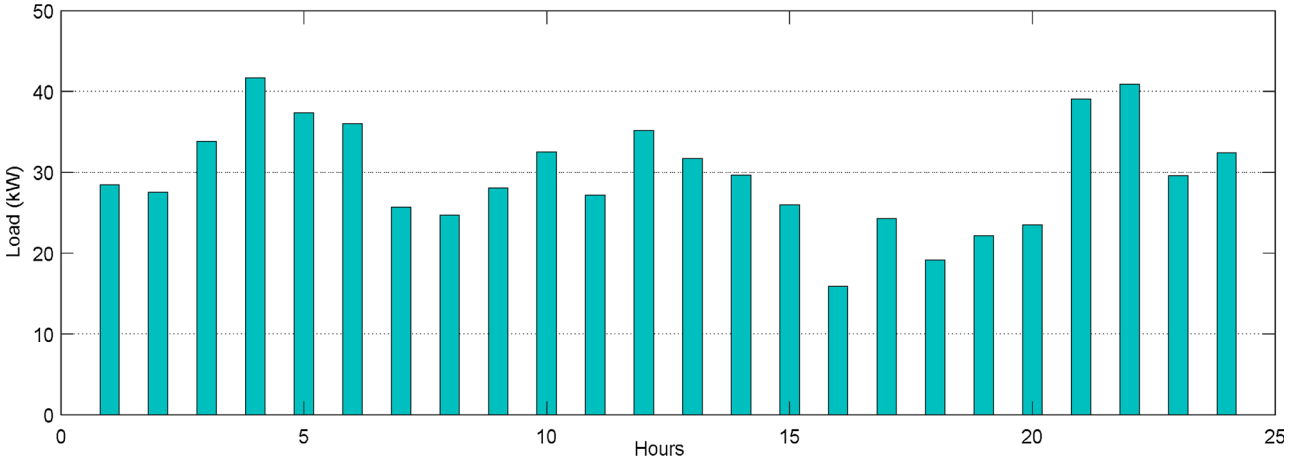

Fig. 2. A full day load demand data of the proposed nanogrid of Danladi Nasidi Quarters.

(a) The wind turbine model

The Equations for power generation in WT obtained in (Atia & Yamada, 2016) are used in the proposed work as Eq. (6) based on specifications for the chosen WT models summarized in Table 4 obtained from a datasheet given in Enercon Energy (2015) Parameters for the wind generation, P_{WT} in watts (W) for a time t from Eq. (6) are v as the general wind speed in m/s, v_{ci} as the cutout speed in m/s, v_{oc} as the cutout speed and v_r as the rated speed. Based on the given Equation three conditions may be considered in obtaining generated power from the WT, P_{WT}. *(i)* P_{WT} may be zero when $v(t)$ is less than v_{ci} or $v(t)$ is greater than v_{co}. *(ii)* P_{WT} may be a fraction of the WT's rated power (P_{rated}) when $v(t)$ is greater than v_{ci} and less than v_r. *(iii)* P_{WT} may be equal to the WT's P_{rated} when $v(t)$ is greater than v_r and less than v_{co}.

$$P_{WT}(t) = \begin{cases} 0, & for\ v(t) < v_{ci}\ \ or\ \ v(t) > v_{co} \\ \dfrac{v^3(t) - V_{ci}^3}{v_r^3 - v_{ci}^3} \times (P_{rated}) & for\ v(t) > v_{ci}\ \ and\ \ v(t) < v_r \\ P_{rated}, & for\ v(t) > v_{ci}\ \ and\ \ v(t) < v_{co} \end{cases} \tag{6}$$

(a) The battery storage system

The main sizing parameters in battery system is the energy storage capacity measured in Ampere-hour (Ah), the terminal open circuit potential in volts (V) expressed in Eq. (7) and the battery type. Lifespan in a battery is mostly determined by the battery's usage and state of charge (SOC) expressed by the constraints defined in Eqs. (8) and (9), where Q_B is the amount of the battery charge, ηP_{ch} is the efficiency based battery charging, PD_{ch} is the battery discharge power, N_B is the battery capacity size and Q_f being the battery charging factor (Table 5).

$$Q_B(t+1) = Q_B(t) + \eta P_{ch}(t) - P_{Dch}(t) \tag{7}$$

$$Q_B(t) \le \overline{SOC} \bullet N_B - Q_f(t) \tag{8}$$

$$Q_B(t) \ge \underline{SOC} \bullet N_B \tag{9}$$

(a) The power converters

The optimal size of an inverter normally corresponds with the RE size (PV and BESS ratings). Voltage produced by PVs and stored by batteries is a direct current (DC) type such that serving alternating (AC) based loads and grid import/export requires inverters, whose operation consumes energy that contributes to losses. This implies that efficiencies are always considered in inverter capacity sizing as specified in Table 6. Hence, Eqs. (10) and (11) for the proposed nanogrid model as obtained in (Atia & Yamada, 2016) describe the constraints upon which the inverter will be specified and operate, where $\eta_{DC/AC}$ and $\eta_{AC/DC}$ are efficiencies of the inverter under DC to AC and AC to DC energy conversion respectively. N_{Inv} is the capacity size of the inverter, P_{Dch} is the charge/discharge power of the battery and P_G is the grid power imports/exports.

$$\eta_{DC/AC}\left[P_{Dch}(t) + P_{PV}(t)\right] \le N_{Inv} \tag{10}$$

$$\eta_{AC/DC}\left[P_{WT}(t) + P_G(t)\right] \le N_{Inv} \tag{11}$$

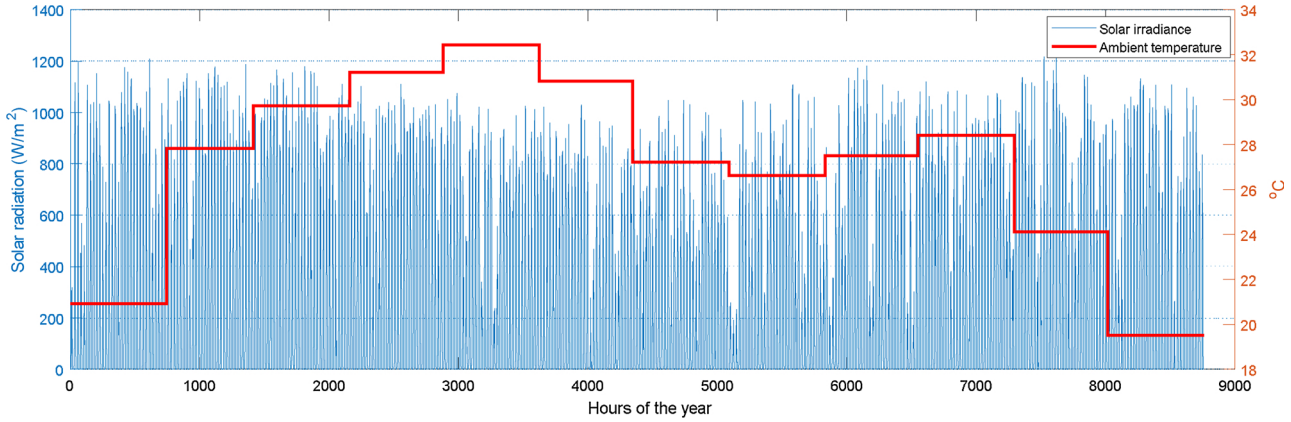

Fig. 3. Annual profile of solar irradiance and ambient temperature for Danladi Nasidi Quarters, Kano, Nigeria.

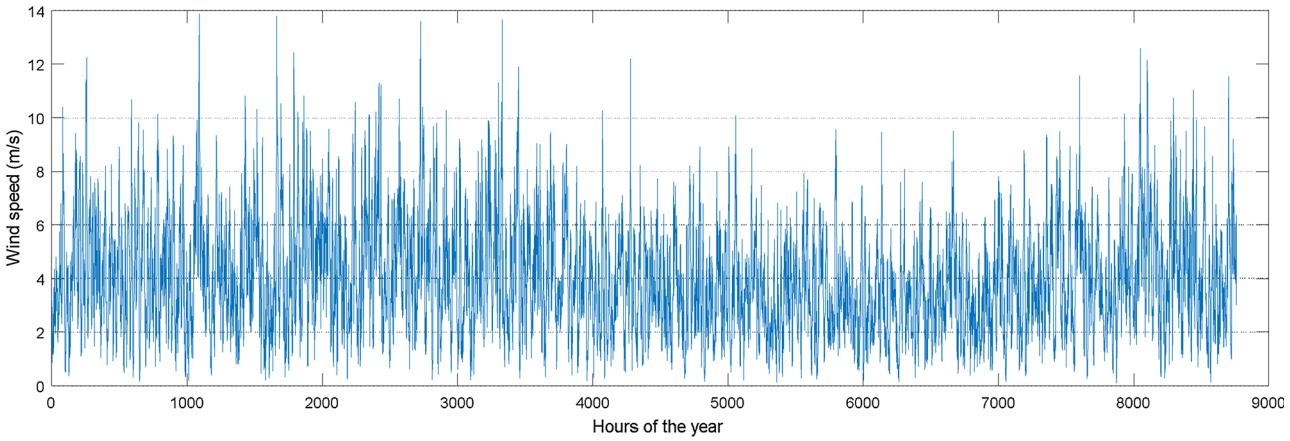

Fig. 4. Annual profile of wind speeds for Danladi Nasidi Quarters, Kano, Nigeria.

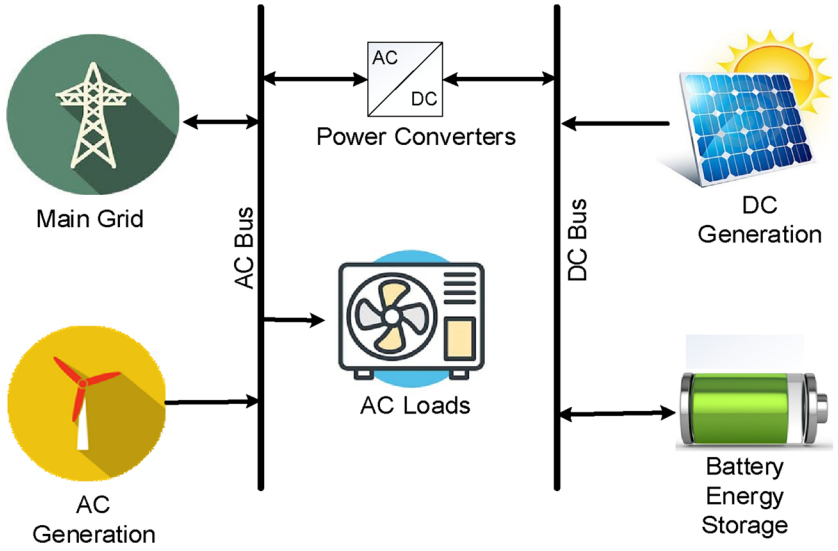

Fig. 5. Proposed nanogrid architecture indicating hybrid energy sources, loads and storage.

Table 3
Specifications and cost data of sampled commercial solar panels (Casey, 2018; Tycon Solar, 2018).

Brands	Power ratings (watts)	Maximum efficiencies	Lifespan (years)	Initial cost/watt ($)	Replacement cost/watt ($)	O&M cost/watt
TPS	30–250	24.3	25	2.86	2.86	0
LG	330–350	20.3	25	3.19	3.19	0
SOLARMO	100–240	18.78	–	1.7	1.7	0.015
Canadian Solar	290–330	18.33	10	3.09	3.09	0
HANHWA Q Cells	290–310	18.1	12	2.94	2.94	0

Table 4
Specifications and cost data of sampled commercial wind turbines (Enercon Energy, 2015).

Brands	Power ratings (kW)	Cut-in speed (m/s)	Rated speed (m/s)	Cut-out speed (m/s)	Lifespan (years)	Initial cost/unit ($)	Replacement cost/unit ($)	O&M cost/unit ($)
Enercon	900	3	10	28	25	137,190	137,190	1,000
Hyundai	1650	3.5	12	20	20	135,500	135,500	1,200
Vestas	3000	3	14	25	25	846,112	846,112	2,500
Siemens	1800	3	13	25	20	150,320	150,320	1,200
Suzlon	2100	3.5	11	25	20	211,400	211,400	1,350

Table 5
Specifications and cost data of sampled commercial energy storage batteries (Victron Energy, 2019).

Brand	Size (Ah)	Terminal rating (V)	η (%)	DoD (%)	Lifespan (years)	Capital cost ($)	Replacement cost ($)	O&M cost
Victron	60	12	98.5	95	7.5	356	356	10
BMZ	120	55	97	80	7	532	532	15
Panasonic	10.6	46.8	90	Auto	10	156	156	10
NEC	35	13.2	70	50	–	322	322	22

Table 6
Specifications and cost data of renewable energy inverters (Solar Edge, 2018).

Brand	Size (kW)	Voltage inputs (v)	η (%)	Voltage outputs (v)	Lifespan (years)	Unit cost ($)	Replacement cost ($)	O&M cost ($)
Solar Edge	20	6	98	230	10	3,384	3,384	250
ABB	3	335-800	96	230	10	14,365	1,365	61
	5	”	96.3	”	”	18,952	1,952	40
	6	”	96.6	”	”	23,056	2,056	103
	10	”	96.6	”	”	28,609	2,609	214
	15	”	96.6	”	”	38,266	3,266	227
	30	”	97	”	”	40,680	4,680	305
	50	”	97	”	”	48,044	4,044	349

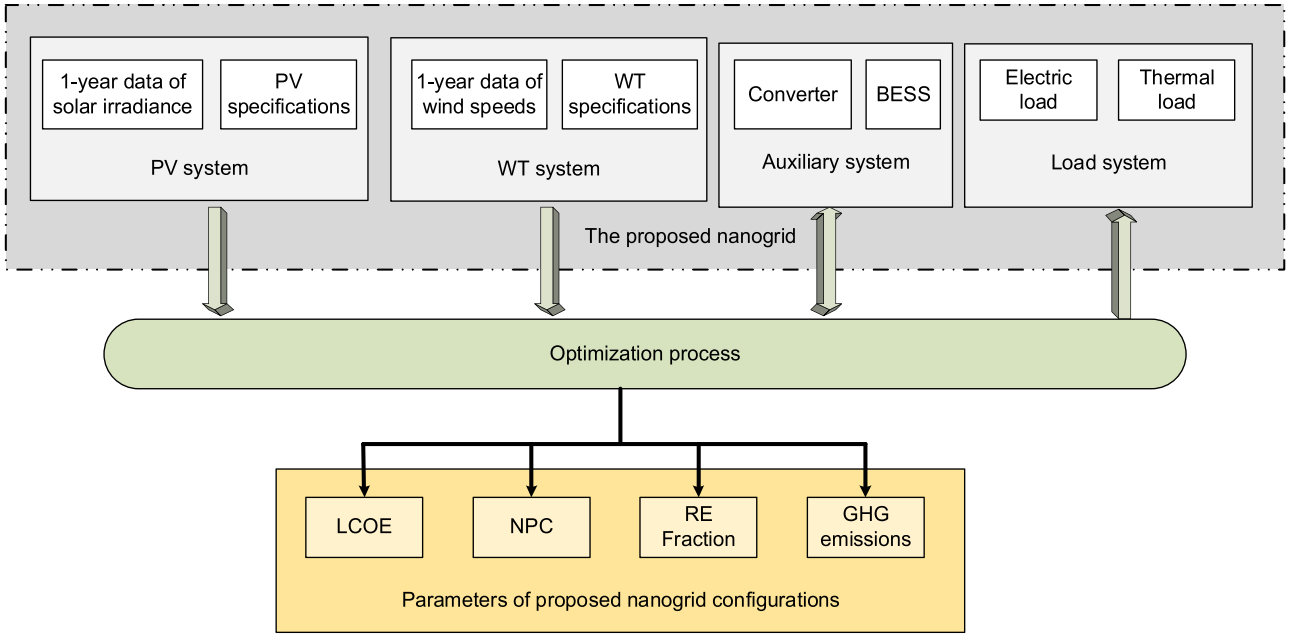

Fig. 6. Implementation of optimizations in the proposed nanogrid using HOMER optimizers.

Table 7
Optimal configurations for components of the proposed nanogrid.

Configurations	PV (kW)	Wind (kW)	Li-ion Battery (kWh)	Converter (kW)
1	150	4500	–	130
2	150	4500	60	130
3	–	4500	–	–
4	–	4500	60	60
5	150	–	–	130
6	150	–	60	130

5. The nanogrid optimized configurations

The components of the nanogrid shown in Fig. 5 have their specifications considered as part of the input parameters to the HOMER optimization system in addition to load and RE resource data. Advantages of using HOMER include robustness in hourly analysis of input data for the purpose of achieving desired optimization objectives based on constraints of energy balance between electric/thermal loads and supply system described in Fig. 6. By implementing a year-long analysis, the method yields several optimal configurations of mainly technical and economic parameters such as the LCOE, LCC, capital cost, replacement cost, operation and maintenance cost, renewable penetration and GHG emissions. Hence, optimization objectives of the proposed nanogrid shown in Fig. 5 may be achieved by simulating the input parameters of weather data, load profiles, RE component specifications and costs provided in Section 3 as described in Fig. 6. Sensitivity analysis can be used to further analyze optimization results on hourly basis due uncertainties of the RE resources and loads. With sensitivity analysis, variation in optimization results may be viewed to reflect corresponding variations of input parameters due to their uncertainties or different range of applications. Different ranges of components specifications were used to produce optimal configurations shown in Table 7. The PV rating (R_P) chosen for the analysis is the 250 W TPS shown Table 3 due to its lower per kW cost of $2.86. From Eqs. (12) and (13), it implies that for 150 kW peak array capacity (P_M)

Table 8
Techno-economic performance parameters of the proposed grid-connected nanogrid.

Configurations	LCOE ($/kWh)	NPC ($)	RE Fraction (%)	GHG Emission (kg/year)	Grid Imports (kWh)	Grid Exports (kWh)
1	−0.0110	−366,210	98	32,463	51,037	2,329,140
2	−0.0110	−365,584	98	32,463	51,037	2,329,140
3	−0.0094	−302,358	97	43,344	68,143	2,138,462
4	−0.0099	−288,680	97	43,344	68,143	2,138,462
5	0.0220	96,852	60	86,716	136,327	112,664
6	0.0222	96,928	60	86,716	136,327	112,664

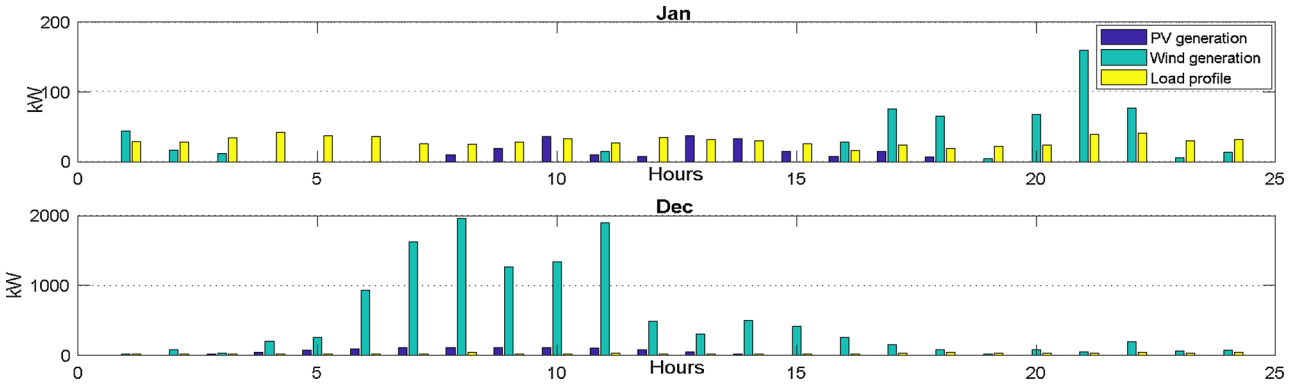

Fig. 7. Hourly power generation and loads for a sampled cold and dry seasonal December/January days.

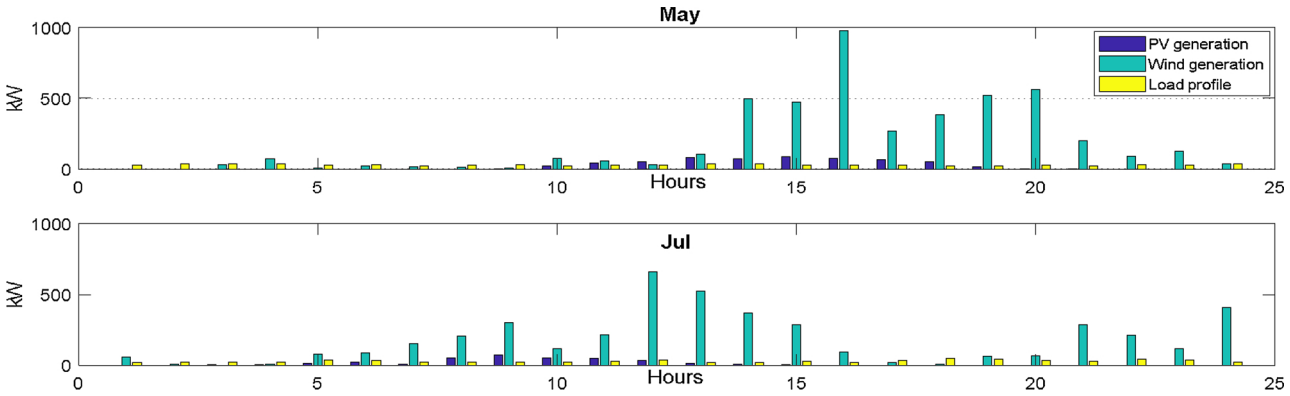

Fig. 8. Hourly power generation and loads for a sampled hot and rainy seasonal May/July days.

to be installed, 600 units of PV modules (N_{PV}) having intrinsic area ($A_{intrinsic}$) of 617.28 m^2 have to be used where based on the module efficiency (η_{PV}) of 24.3% and standard solar irradiance I_{ST} of 1000 W/m^2. The Enercon WT systems used have 900 kW rated capacity which requires 5 units to be installed, that is average of 1 unit per housing unit. Victron having the second lowest price per unit Ampere-hour (Ah) of $5.93 is the battery chosen for the analysis. The preference for Victron is that it has higher efficiency and DoD of 98.5% and 95% against the cheapest analyzed BMZ battery's efficiency and DoD of 97% and 80% respectively. Similarly, Solar Edge inverters have more advantage in terms of cost and efficiency of $169.20 and 98% against range of ABB inverters with lowest price of $960.88 and highest efficiency of 97%.

$$N_{PV} = \frac{P_M}{R_P} \tag{12}$$

$$A_{intrinsic} = \frac{P_M}{I_{ST} \times \eta_{PV}} \tag{13}$$

The PV and wind system considered were analyzed based on available wind speeds and solar irradiance and load profiles of the location shown in Figs. 3 and 4. The system was simulated at 6% and 5% interest and discount rates respectively under 0.01 design precision and projected to last 25 years (Fig. 6). Top six configurations are considered for analysis based on their optimality ranking and discussed in the following section. The remaining configurations exhibits annualized characteristics of high energy imports and nothing to export which may be feasible but not optimal to be preferred in the analysis going by the trend where increase in imports and corresponding decrease in exports affect the values of LCOE and NPC as indicated in Table 8.

6. Optimization results, analyses and discussions

The optimization results of the autonomous nanogrid discussed in (Akinyele, 2017) were set to be used to compare the performance of the proposed nanogrid in both reliability and economy. The 70% renewable penetration realized in the reference study is being adequate however, the LCOE of 0.689 $/kWh needs to be reduced to some values much lower than the retail rates of 0.6 $/kWh. One other important issue to be considered is that the autonomous system has dump energies due to unused RE generation especially when the maximum SOC of BESS are reached. Hence, the proposed nanogrid takes dump energy into consideration and suggests grid trade-offs so that the excess generation can be exported to the grid to increase system's economic performance. In HOMER, a resistive heater is usually employed to convert the excess

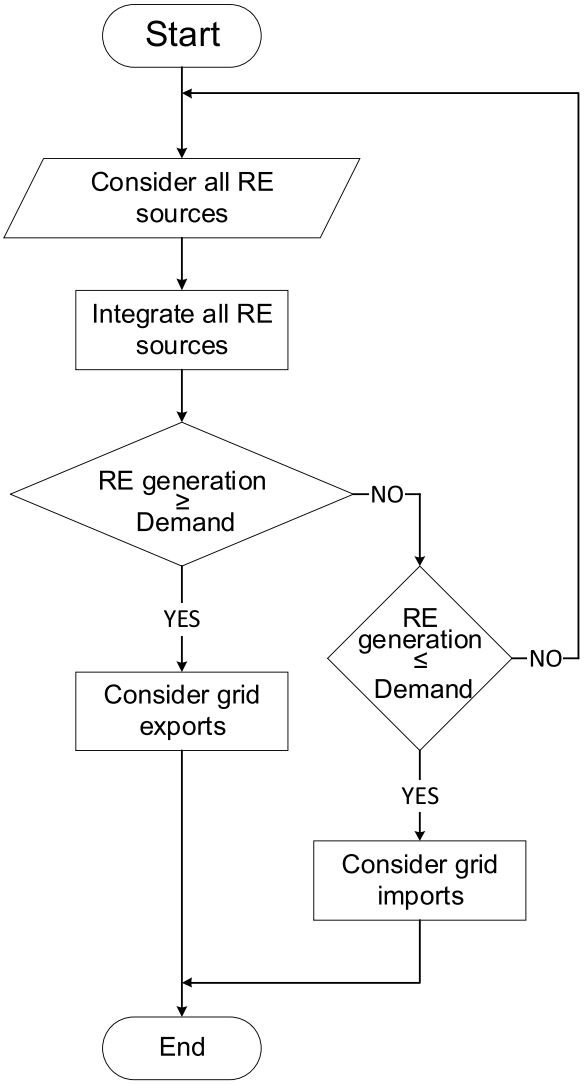

Fig. 9. Flowcharts describing algorithms for the proposed nanogrid operation.

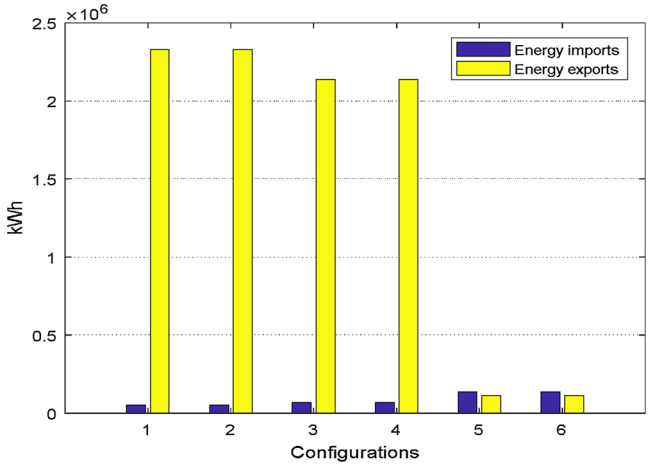

Fig. 10. Annualized energy trade-offs under different configurations of the proposed nanogrid.

energy into thermal load using "Thermal Load Controller" HOMER ENERGY (2019). Since the proposed nanogrid architecture consists of grid connection, economically it becomes imperative to use grid as a dump load for absorbing the excess energy. Optimization results of the

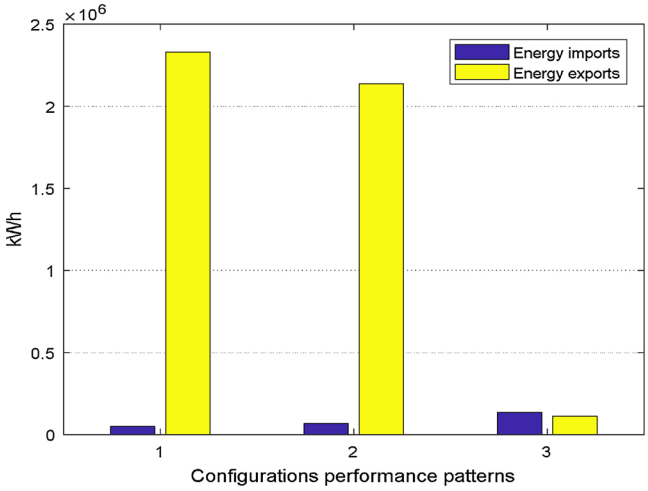

Fig. 11. Three identical energy annualized trade-offs of the nanogrid configurations.

proposed system being presented in Table 8 shows six topmost optimal configurations each with performance parameters being obtained. It is worthy of note that the parameters realized determines systems' configuration to be chosen depending on the set objective functions, which are all tied to the grid utilities.

(a) Configurations 1 & 2

Configuration 1 is the highest optimal settings obtained from the system comprising of a 150 kW of PV, 4500 kW of WT and 130 kW inverter. The inverter size is determined from Eqs. (10) and (11) indicating that power losses in inverter circuits contributes to inefficiencies. Table 6 shows that the lowest inverter efficiency is 96% however, only 86.67% (130 kW) of the 150 kW PV rating is considered as lowest and feasible inverter size in the proposed configurations, which is the same as 1.154 array-to-inverter ratio, that falls within the range (1.15 to 1.25) recommended in (Thoubboron, 2018). This configuration exhibits large potentials for energy export to the grid which implies much lower LCOE and NPC comparatively. The RE fraction of 98% is much adequate to be compared with many configurations of autonomous or grid-connected systems. The −0.0110 $/kWh cost of energy implies a corresponding positive gain of 0.0110 $/kWh by the nanogrid for every kW generated and exported. This configuration also has a comparatively low GHG emission rates. Configuration 2 differs from configuration 1 only for the addition of 60 kW h BESS capacity. The only parameter being affected by the change is the NPC with difference of $626 (−$366,210 in configuration 1 compared to −$365,584 in configuration 2) for an annualized sum where the first configuration has better advantage.

(b) Configurations 3 & 4

There are peculiarities within configurations 3 and 4 from the six optimal solutions realized. The two configurations (3 & 4) consider only WT as the only source of RE generation to be used by the nanogrid. Thus, under these configurations grid exports are still high, implying that a corresponding low grid imports, negative values of LCOE and NPC (−0.0094 $/kWh and −$302,358 respectively) can be maintained that may have to require functional FIT to be implemented (Fendri & Chaabene, 2019). The RE fraction of 97% is maintained in the two configurations however, there is an appreciable growth in the GHG emission against the first two sets of configurations. The system components in the fourth configuration differ from the third configuration only in the use of 60 kW h BESS. The gain in the LCOE of 0.0001 $/kWh (−$0.0094 to −$0.0095)kWh was insignificant, whereas the system

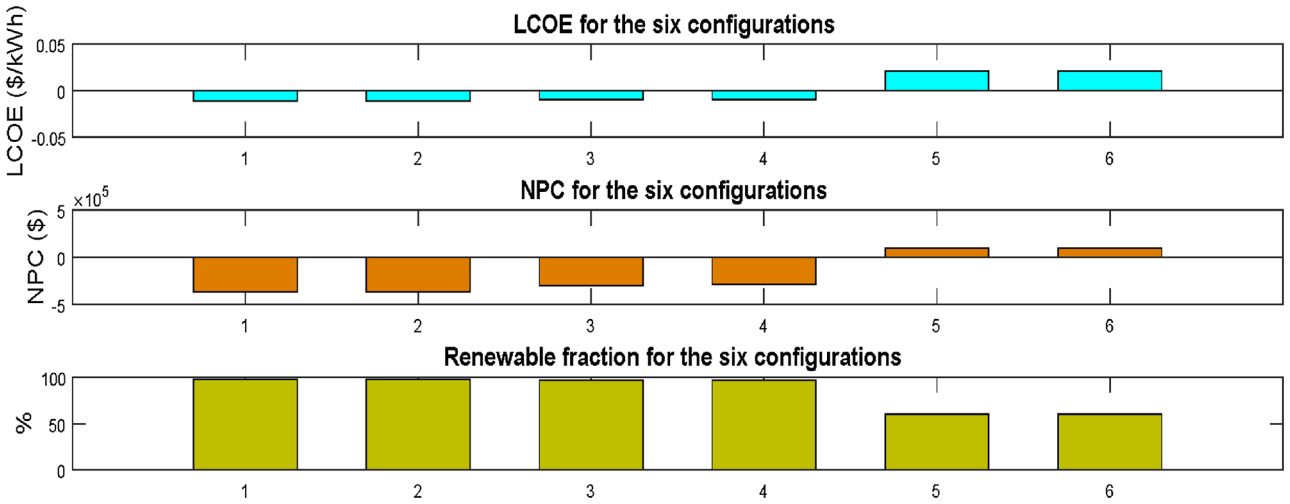

Fig. 12. Techno-economic performance analysis of the proposed nanogrid.

value reduced by $13,678 (NPC changes from −$302,358 to −$288,680). These arrangements have a feasible solution but, with a comparatively lower benefits than the first two configurations. The GHG emission is high however, grid export and import levels are adequate for the configurations to maintain negative values of both LCOE and NPC.

(c) Configurations 5 & 6

Although fifth in the feasibility ranking, configuration 5 is the first configuration to have a positive value of LCOE and NPC. The change corresponds to grid imports that exceed the exports. This is another optimal configuration whose contribution to grid maintains a low LCOE as compared to the current grid tariff rates of 0.6 $/kWh. The positive values of LCOE and NPC indicate the aggregate energy cost to be borne by the nanogrid per each kW generated. The configuration only considers PV for RE penetration hence, RE fraction in this case dropped to 60%. In configuration 6, values for RE fraction, GHG emission, grid exports and imports did not differ from the fifth configuration. The PV only grid-connected system of configuration 5 added a 60 kW h storage capacity. The addition causes increase in LCOE by 0.0002 $/kWh that appear insignificant although NPC increased by $76. The much lower LCOE realized in the six configurations are only but average values for electricity cost for a year-long operation. Hence, LCOE values may differ periodically based on operational conditions of the system instantaneously. Optimal EM objectives for generating components' dispatch and load scheduling can be useful to improve economic performance analysis and realistic time of use tariffs (Khalkhali & Hosseinian, 2019).

The six configurations exhibit appreciable RE penetrations of 60 to 98% that is adequate to highly rate the nanogrid performance. The wind contributes close to 91% of the total RE generation, while 9% of PV contribution may insignificantly be considered in system configurations however, there are periods of wind power loss as shown in Figs. 7 and 8 (when actual wind speeds are lower than WT's design cut-in speed) upon which the nanogrid may be used to improve the system reliability based on Eq. (6) with respect to wind profiles of Fig. 4. The constraints of limited space for the PV array and needs for promotion of RE system of power generation and utilization due to free inexhaustible fuels is another deciding factor for such combinations. Moreover, it is unlikely that the 4500 kW capacity of the WT could be fully achieved (even when the wind speeds are above cut-in speed) due to the WT's capacity factor that hardly exceeds 0.4 (40% of the installed capacity) (Khalkhali & Hosseinian, 2019). The envisaged prospects for energy tradeoffs indicated in Fig. 10 shall be feasible through functional system operations to be implemented by optimization algorithms described in the flow chart of Fig. 9, where the system initially considers RE sources first for primary consumption and storage. Any excess generation may be exported to the main grid. In any event of supply deficits from the primary (RE) sources and storage, the system hence considers imports from main grid. Storage hidden in the flow chart may be considered for duality purpose hence, during charging period categorized as load and during discharge as part of RE sources being integrated to serve the load and possibly grid exports.

7. Summary

A critical look into results presented in Table 8, indicates that the six configurations exhibits three different techno-economic performance patterns, where each pair of configurations discussed in Section 6 have identical performance patterns and components structures (consider Tables 7 & 8 and Figs. 10 & 11). Configurations 1 and 2 have both PVs and wind as RE components. Storage makes the only difference hence the two configurations may be classified within the first pattern. The pattern may be more clearly expressed by analyzing the optimization results, which showcases the LCOE, RE fraction, GHG emission and grid exports and imports apart from NPC having exactly the same values. The second pattern utilized only wind in RE generation. The pattern is conceived through comparison between the third and fourth configurations in terms of component structures. The only difference within this performance pattern (involving third and fourth configurations) is the 60 kW h converter and storage in the fourth configuration aimed to be utilized during hours of autonomous operations. The optimization results also show the difference only lies in the NPC values. The third pattern which comprises of fifth and sixth configurations had PVs as the only RE generating components. Like the two previous patterns, storage is the only difference between the two configurations making up the third pattern. Figs. 10 and 11 consider grid exports and imports in both configuration and patterns as the main parameters considered in feasibility analysis for the proposed nanogrid. Four out of six configurations shown in Fig. 12 are negative value of LCOE and NPC, indicating potentials for grid exports. Inclusion of Li-ion battery storage

contributes insignificantly to lower LCOE and NPC objectives (Bachner et al., 2017; Ueckerdt et al., 2013). Despite the insignificant economic contribution from the battery, it is however important for reliability enhancement against main grid failures and uncertainties of the weather conditions (Sharifi & Maghouli, 2018).

8. Conclusions

There are methods used in optimizations for sizing and operations of modern electric power grids. Software based optimization methods are used in achieving multiple optimization objectives due to their speed and versatility. Efforts to consolidate gains of a RE-based autonomous nanogrid implemented in HOMER were achieved by substituting diesel plants used in the reference case with a main grid connection in a proposed study with the aim of improving the 150 kWh per capita electricity consumption and relatively higher LCOEs and NPCs of the reference case. Several optimal configurations of nanogrid components were realized hence, the four topmost optimal configurations had LCOE ranges 0.0095 $/kWh to 0.0110 $/kWh, and NPC ranges $288,680 to $366,210. Fifth and sixth configurations have LCOEs as 0.0220 $/kWh and 0.0222 $/kWh as well as NPCs of $96,852 and $96,928 respectively. The nanogrid's RE penetration were 98%, 97% and 60% for the six configurations. The nanogrid achieved a moderately lower emission of 2328 tons/year as compared to 4000 tons/year in the reference case. The negative values of LCOEs and NPCs obtained in the first four configurations indicates high prospects for the proposed nanogrid's energy exports to the main grid. The feasibilities of the configurations suggest potentials for improving the per capita electricity consumption within the area of study through RE-based systems in addition to the system's contribution to clean energy production. The renewable penetration and the emission rates of the proposed nanogrid may require legislative support and operational incentives. It is therefore suggested that the optimization results obtained can further be consolidated through integrations of functional FIT into the system operations.

Acknowledgement

The authors want to acknowledge generosity of the management of Federal College of Education (Technical) Bichi, Kano State, Nigeria for the In-service programme offered to the first author through Tertiary Education Trust Fund (TETfund) intervention. The authors also acknowledge the Universiti Teknologi Malaysia's International Doctoral Fellowship (IDF) assistance offered to the first author in addition to conducive environments for learning and research in terms of laboratories, libraries and social amenities.

References

Abdilahi, A. M., Mohd Yatim, A. H., Mustafa, M. W., Khalaf, O. T., Shumran, A. F., & Mohamed Nor, F. (2014). Feasibility study of renewable energy-based microgrid system in Somaliland's urban centers. *Renewable and Sustainable Energy Reviews, 40*, 1048–1059.

Akinyele, D. (2017). Techno-economic design and performance analysis of nanogrid systems for households in energy-poor villages. *Sustainable Cities and Society, 34*(July), 335–357.

Akmal, M., El Kashif, A., Ghazal, M., & Al Tarabsheh, A. (2016). Demand response enabled sustainable smart home design in the middle east environment. *EEEIC 2016 - Int. Conf. Environ. Electr. Eng.*

Akram, U., Khalid, M., & Shafiq, S. (2018). An improved optimal sizing methodology for future autonomous residential smart power systems. *IEEE Access, 6*.

Atia, R., & Yamada, N. (2016). Sizing and analysis of renewable energy and battery systems in residential microgrids. *IEEE Transactions on Smart Grid, 7*(3), 1204–1213.

Ayop, R., Isa, N. M., & Tan, C. W. (2018). Components sizing of photovoltaic stand-alone system based on loss of power supply probability. *Renewable and Sustainable Energy Reviews, 81*(May 2016), 2731–27312743.

Bachner, G., Tuerk, A., Williges, K., & Steininger, K. (2017). *D4.2 Economic costs and benefits of renewables deployment in the EU.* no. January48.

Ban, M., Shahidehpour, M., Yu, J., & Li, Z. (2017). A cyber-physical energy management system and optimal sizing of networked nanogrids with battery swapping stations. *IEEE Transactions on Sustainable Energy, 3029*(c), 1–11.

Borhanazad, H., Mekhilef, S., Gounder Ganapathy, V., Modiri-Delshad, M., & Mirtaheri, A. (2014). Optimization of micro-grid system using MOPSO. *Renewable Energy, 71*, 295–306.

Boussetta, M., El Bachtiri, R., Khanfara, M., & El Hammoumi, K. (2017). Assessing the potential of hybrid PV–Wind systems to cover public facilities loads under different Moroccan climate conditions. *Sustainable Energy Technologies and Assessments, 22*, 74–82.

Burmester, D., Rayudu, R., Seah, W., & Akinyele, D. (2017). A review of nanogrid topologies and technologies. *Renewable and Sustainable Energy Reviews, 67*, 760–775.

Casey, B. (2018). *Solar panel ratings explained – Solaris.* [Online]. Available: https://www.solaris-shop.com/blog/solar-panel-ratings-explained/. (Accessed: 02-Jul-2019).

E. (International R. E. A.-I. Aberg, et al. (2018). *17-8652_GSR2018_FullReport_web_-1*.

Enercon Energy (2015). *ENERCON product overview.* [Online]. Available: https://www.enercon.de/fileadmin/Redakteur/Medien-Portal/broschueren/pdf/en/ENERCON_Produkt_en_06_2015.pdf. (Accessed: 30-Jan-2019).

Fendri, D., & Chaabene, M. (2019). Hybrid Petri Net scheduling model of household appliances for optimal renewable energy dispatching. *Sustainable Cities and Society, 45*(November 2018), 151–1512158.

HOMER ENERGY (2018). *Net present cost.* [Online]. Available: https://www.homerenergy.com/products/pro/docs/3.11/net_present_cost.html. (Accessed: 23-Dec-2018).

HOMER ENERGY (2019). *Excess electricity.* [Online]. Available: https://www.homerenergy.com/products/pro/docs/3.11/excess_electricity.html. (Accessed: 29-Jun-2019).

Honsberg, C., & Bowden, S. (2019). *Calculation of solar insolation.* PVEducation [Online]. Available: https://www.pveducation.org/pvcdrom/properties-of-sunlight/calculation-of-solar-insolation. (Accessed: 06-Jul-2019).

Hussain, A., Arif, S. M., Aslam, M., & Shah, S. D. A. (2017). Optimal siting and sizing of tri-generation equipment for developing an autonomous community microgrid considering uncertainties. *Sustainable Cities and Society, 32*(April), 318–330.

International Renewable Energy Agency (2014). *Overview of solar and wind maps.* 50.

Isa, N. M., Das, H. S., Tan, C. W., Yatim, A. H. M., & Lau, K. Y. (2016). A techno-economic assessment of a combined heat and power photovoltaic/fuel cell/battery energy system in Malaysia hospital. *Energy, 112*, 75–90.

Jacob, A. S., Banerjee, R., & Ghosh, P. C. (2018). Sizing of hybrid energy storage system for a PV based microgrid through design space approach. *Applied Energy, 212*(September 2017), 640–6402653.

Khalkhali, H., & Hosseinian, S. H. (2019). Novel residential energy demand management framework based on clustering approach in energy and performance-based regulation service markets. *Sustainable Cities and Society, 45*(November 2018), 628–6282639.

Li, B., Roche, R., Paire, D., & Miraoui, A. (2017). Sizing of a stand-alone microgrid considering electric power, cooling/heating, hydrogen loads and hydrogen storage degradation. *Applied Energy, 205*(September), 1244–1259.

Liu, Z., Chen, Y., Zhuo, R., & Jia, H. (2017). Energy storage capacity optimization for autonomy microgrid considering CHP and EV scheduling. *Applied Energy, 210*, 1113–1125.

Mallol-Poyato, R., Jiménez-Fernández, S., Díaz-Villar, P., & Salcedo-Sanz, S. (2017). Adaptive nesting of evolutionary algorithms for the optimization of Microgrid's sizing and operation scheduling. *Soft Computing, 21*(17), 4845–4857.

Momoh, J. (2012). *SMART GRID: Fundamentals of design and analysis.* Hoboken, New Jersey: Institute of Electrical and Electronics Engineers, John Wiley & Sons, Inc.

Paper, O., & Boer, D. (2013). *Review on for review only.* 0–34.

Rahbari, O., et al. (2017). An optimal versatile control approach for plug-in electric vehicles to integrate renewable energy sources and smart grids. *Energy, 134*, 1053–1067.

Sadati, S. M. S., Jahani, E., Taylan, O., & Baker, D. (2017). Sizing of PV-wind-battery hybrid system for a Mediterranean Island community based on estimated and measured meteorological data. *Journal of Solar Energy Engineering, 140*(February), 1–12.

Sadati, S. M. S., Jahani, E., Taylan, O., & Baker, D. K. (2018). Sizing of photovoltaic-wind-battery hybrid system for a Mediterranean Island community based on estimated and measured meteorological data. *Journal of Solar Energy Engineering, Transactions of the ASME, 140*(1), 1–12.

Sepulveda, S. R., Camilo, C. L., & Mauricio, S. (2018). Methodology for ESS-type selection and optimal energy management in distribution system with DG considering reverse flow limitations and cost penalties. *IET Generation, Transmission & Distribution, 12*(5), 1164–1170 (6).

Sharifi, A. H., & Maghouli, P. (2018). Energy management of smart homes equipped with energy storage systems considering the PAR index based on real-time pricing. *Sustainable Cities and Society, 45*(December 2018), 579–587.

Solar Edge (2018). *Three phase inverters.* [Online]. Available: http://www.solaredge.com/files/pdfs/products/inverters/se-three-phase-us-inverter-208V-datasheet.pdf. (Accessed: 30-Jan-2019).

Strnad, I., & Prenc, R. (2017). Optimal sizing of renewable sources and energy storage in low-carbon microgrid nodes. *Electrical Engineering, 100*(3), 1661–1674.

Sukumar, S., Mokhlis, H., Mekhilef, S., Naidu, K., & Karimi, M. (2017). Mix-mode energy management strategy and battery sizing for economic operation of grid-tied microgrid. *Energy, 118*, 1322–1333.

Thoubboron, K. (2018). *How does solar inverter sizing work?* EnergySage [Online]. Available: https://news.energysage.com/what-size-solar-inverter-do-i-need/.

(Accessed: 01-Sep-2019).
Tudu, B., Mandal, K. K., & Chakraborty, N. (2018). *Optimal design and development of PV-wind-battery based nano-grid system: A fi eld-on-laboratory demonstration*.
Tycon Solar (2018). *Heavy duty solar panels TPS-W series TPS-12-80W and TPS-12-30W and TPS12-10W 12V 80W, 30W and 10W panels TPS-12-80W TPS-12-30W TPS-12-10W.* [Online]. Available: https://tyconsystems.com/documentation/Spec Sheets/TPS-W Solar Panels Spec Sheet.pdf. (Accessed: 30-Jan-2019).
Ueckerdt, F., Hirth, L., Luderer, G., & Edenhofer, O. (2013). System LCOE: What are the costs of variable renewables? *Energy, 63*, 61–75.
Victron Energy (2019). *Gel and AGM batteries.* [Online]. Available: www.victronenergy.com. (Accessed: 30-Jan-2019).
Zenginis, I., Vardakas, J. S., Echave, C., Morató, M., Abadal, J., & Verikoukis, C. V. (2017). Cooperation in microgrids through power exchange: An optimal sizing and operation approach. *Applied Energy, 203*(April), 972–981.